Chapter 2
Metal–Dielectric Diffusion Processes: Fundamentals

There are two main mechanisms by which metal species can migrate into dielectrics. One is *diffusion* of metal atoms at an elevated temperature driven by the metal concentration gradient. The other is *drift* of metal-ions as a result of an external electric field. In the latter case, metal-ions have to be generated at the metal–dielectric interface for the drift to begin [1]. The origin of metal-ion generation is related to the chemical interaction between the metal and the dielectric at their interface. For example, a metal oxide may be formed if there is an oxidant residing at the interface. In this chapter, we attempt to describe a coherent treatment of ion generation and drift based on the thermochemistry that occurs at the metal–dielectric interface. The basic formulation of atomic diffusion and ionic drift is reviewed.

2.1 Thermal Diffusion

Ideally, when metal atoms are brought into contact with a dielectric surface, the interface is very sharp, as shown schematically in Fig. 2.1a. However, under sufficiently high temperature, metal atoms can be activated so that they undergo a random walk from site to site at the interface. Since the concentration of the metal atoms within the deposited metal film is much larger than that in the dielectric, this movement produces a net flow of metal atoms across the interface into the dielectric. As a consequence, the boundary between the metal and the dielectric is no longer clearly defined, as shown in Fig. 2.1b.

In one dimension, the net flux of metal atoms inside a dielectric film is given by Fick's first law [2]:

$$f(x,t) = -D\frac{\partial \rho(x,t)}{\partial x}, \tag{2.1}$$

M. He and T.-M. Lu, *Metal-Dielectric Interfaces in Gigascale Electronics*, Springer Series in Materials Science 157, DOI: 10.1007/978-1-4614-1812-2_2,

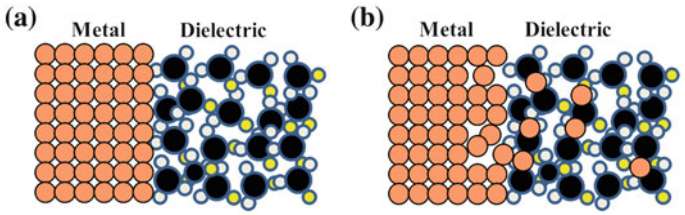

Fig. 2.1 A schematic diagram showing the interface between the metal and dielectric materials. **a** An ideal sharp interface prior to diffusion, and **b** a diffused interface after the penetration of the metal into the dielectric

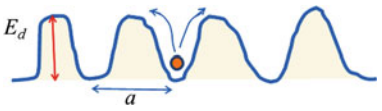

Fig. 2.2 A schematic diagram showing the motion of an atom in a diffusion process through a potential energy barrier E_d. The site-to-site distance is denoted by a (on the order of several angstroms)

where f is the flux, defined as the number of metal atoms passing through a unit cross-sectional area per unit time, ρ is the concentration of metal atoms in a unit of cm^{-3}, and $\partial\rho(x,t)/\partial x$ is the concentration gradient (the driving force for diffusion). The position x is measured from the interface toward the dielectric. D is the diffusion coefficient, or the diffusivity in unit of cm^2/s. The diffusion of metal atoms inside a dielectric is a thermally activated process, as shown in Fig. 2.2. The diffusivity can be written as an Arrhenius form:

$$D = D_0 e^{-E_d/k_B T}, \tag{2.2}$$

where D_0 is the pre-exponential factor. E_d is the potential energy barrier height for the atom motion inside a dielectric (on the order of electron volts), k_B is the Boltzmann constant, and T is the temperature. Equation (2.2) can be applied to all species that are in motion. If ions are the moving species, then E_d is the barrier height for the ion motion.

Fick's first law basically says that flux is proportional to the concentration gradient. The concentration may change as a function of time during the diffusion process. The mass balance requirement gives Fick's second law [2]:

$$\frac{\partial\rho(x,t)}{\partial t} = -\frac{\partial f(x,t)}{\partial x} = \frac{\partial}{\partial x}\left(D\frac{\partial\rho(x,t)}{\partial x}\right). \tag{2.3}$$

If D is independent of x, which is a valid assumption when the metal concentration inside a dielectric is dilute, then Eq. (2.3) can be simplified as

$$\frac{\partial \rho(x,t)}{\partial t} = D\frac{\partial^2 \rho(x,t)}{\partial x^2}. \tag{2.4}$$

In this equation, the most important parameter to describe atomic diffusion is the diffusivity, D. The higher the diffusivity, the faster an atom can migrate inside the dielectric. It is therefore essential to obtain this coefficient in order to understand the behavior of metal transport inside a dielectric. The diffusivity is usually evaluated by solving Eq. (2.4) numerically with the actual boundary conditions.

Under certain boundary conditions, Eq. (2.4) can be solved analytically. For most of the diffusion experiments discussed in this monograph, all test samples have a thick layer (hundreds of nanometers) of metal deposited on the dielectric, serving as a constant diffusion source. Assuming that the annealing process has not driven metal atoms across the whole dielectric film to reach the other interface, an analytical solution for Eq. (2.4) can be derived. It is called the predeposition diffusion, with the boundary conditions described below:

$$\begin{aligned} &\rho(x, t = 0) = 0 \\ &\rho(x = 0, t) = \rho_s. \\ &\rho(x = d, t) = 0 \end{aligned} \tag{2.5}$$

Here, ρ_s is the fixed metal concentration at the metal–dielectric interface, and d is the dielectric thickness. The solution of Eq. (2.4) with these boundary conditions is

$$\rho(x,t) = \rho_s\left(1 - \mathrm{erf}\left(\frac{x}{2\sqrt{Dt}}\right)\right). \tag{2.6}$$

In this equation, $\sqrt{Dt}$ is the characteristic diffusion depth, and erf is the error function, defined as $\mathrm{erf}(x) = \frac{2}{\sqrt{\pi}}\int_0^x e^{-t^2}dt$. The surface concentration ρ_s can be obtained by an elemental measurement. By fitting the profile from Eq. (2.6) with the distribution data from elemental characterization, the only variable, D, can be estimated. If both sides of Eq. (2.6) are divided by the surface concentration ρ_s, the relative concentration profile is given by

$$\frac{\rho(x,\, t)}{\rho_s} = 1 - \mathrm{erf}\left(\frac{x}{2\sqrt{Dt}}\right). \tag{2.7}$$

This equation is more suitable for fitting the depth profile obtained from elemental measurements, most of which only provide the information of relative counts instead of actual concentration data. As an example, based on Eq. (2.7), relative concentration profiles are plotted as a function of diffusion depth for the predeposition diffusion in Fig. 2.3. Both diffusivity and annealing time can contribute to diffusion length.

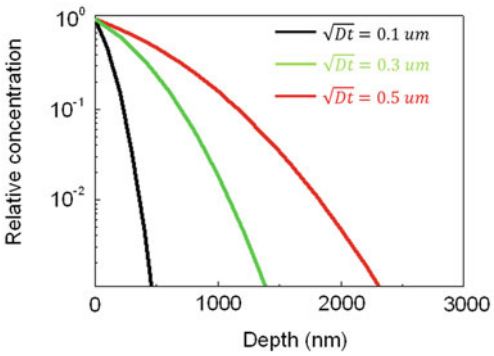

Fig. 2.3 Relative concentration profiles are plotted as a function of diffusion depth for predeposition diffusion

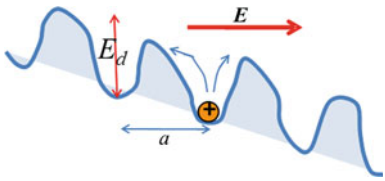

Fig. 2.4 A schematic diagram showing the motion of an ion in an activated process through a potential energy barrier E_d and an external electric field E. The potential is tilted to the right, enhancing the ion drift

2.2 Field-Enhanced Ion Drift

The situation can be very different if a strong electric field is applied to the dielectric and there are ions, instead of atoms, inside the dielectric. When this occurs, the electric field will provide an additional driving force for ion migration inside the dielectric. Figure 2.4 is a schematic diagram showing the motion of an ion in a dielectric film under the influence of an external electric field. Effectively, the external electric field will tilt potential barriers towards the right, causing the ions to drift more easily to the right, particularly if the sample is stressed at an elevated temperature. The flux to the right has a drift term due to the electric field, in addition to the thermal diffusion term given by Eq. 2.1 [3]:

$$f(x,t) = -D\frac{\partial\rho(x,t)}{\partial x} + \frac{qDE(x,t)\rho(x,t)}{kT}, \tag{2.8}$$

where q is the electric charge, and $E(x,t)$ is the effective electric field, which includes both the external field and the ionic field from the penetrated ions. Here D represents the metal-ion diffusivity and is independent of the location inside the dielectric if the ion concentration is limited [4]. This equation is valid when the electric field is relatively small ($E \ll kT/qa$, where a is the lattice spacing). This condition is satisfied under most testing conditions discussed in this monograph. A more general description of the ionic flux is given by [3, 5]:

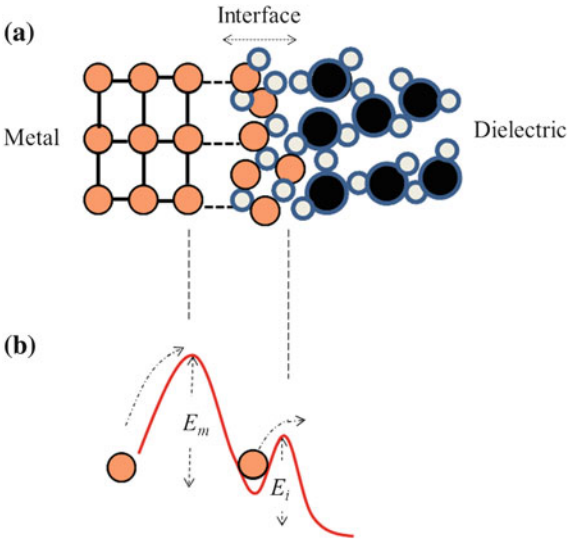

Fig. 2.5 **a** An atomistic scale schematic of the metal–dielectric interface. **b** An energy diagram showing how metal atoms diffuse out of the metal matrix into the dielectric. Metal atoms need to overcome two barriers in order to diffuse into the dielectric film, including the metallic bonding with metal matrix and the barrier from the interface layer

$$f(x,t) = -D\cosh\left(\frac{qaE}{2kT}\right)\frac{\partial\rho(x,t)}{\partial x} + \frac{2D}{a}\sinh\left(\frac{qaE}{2kT}\right)\rho(x,t). \tag{2.9}$$

This equation takes into account the lowering of the diffusion energy barrier by the external electric field. Such barrier lowering effect needs to be considered if testing is carried out at an extreme condition, for example, at 400°C with an E field in the MV/cm range.

Ion diffusivity can also be estimated in a similar way as is done in atomic diffusion, by simulating the distribution profile using Eq. (2.8) or (2.9) in Fick's second law, which can be solved numerically. In addition to elemental characterizations, there are other ways such as electrical methods that one can employ to derive metal-ion diffusivity, which will be discussed in Chap. 8.

2.3 Thermodynamics and Chemical Interactions

The discussion above focuses on the migration behavior of atoms and ions inside dielectrics, but the process by which these metal atoms or ions are initially released from the metal into the dielectric is actually quite complex.

For metal atoms to thermally diffuse into a dielectric, the atoms need to overcome metallic bonding (E_m) with the rest of the metal matrix, as shown in Fig. 2.5. A good indication of metallic bonding strength (E_m) is given by the melting point of the material. A higher melting temperature corresponds to a stronger bonding energy within the metal matrix; therefore, it is generally more difficult for a metal with a higher melting temperature to be released from its metal

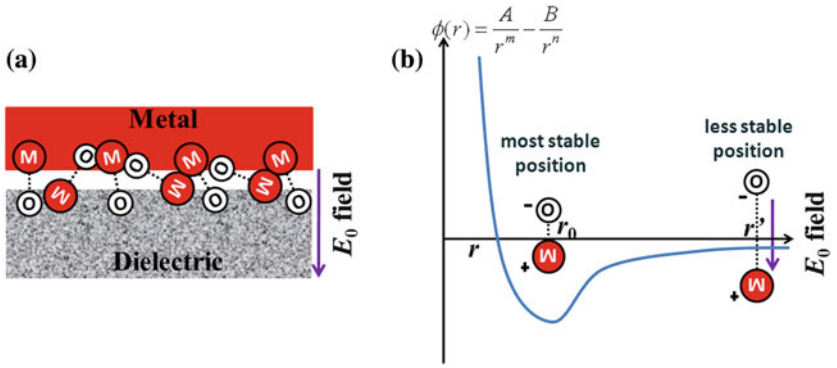

Fig. 2.6 **a** A schematic of M–O bonds at the metal–dielectric interface. **b** The Mie-GrÜneisen potential energy of M–O bonding. Without an external electric field, the length of M–O bond is at the most stable position, r_0. The torque from the external field will stretch the M–O bond and the bond will deviate away from its most stable position

matrix into the dielectric. The melting points of different metals can be found in Fig. 1.5. Meanwhile, there may also be an interface layer that is the product of the surface reaction between the metal and the dielectric film, as shown in Fig. 2.5a. This interface layer will add another energy barrier (E_i) that must be overcome before metal atoms can penetrate the dielectric, as shown in Fig. 2.5b. The barrier strength depends upon the chemistry and film quality of the interface layer.

The origin of metal-ions depends on the chemistry of the interface layer. Many dielectric materials used in electronic devices contain oxygen [6]. The oxidation of the metal at the dielectric surface is perhaps the most important reaction that can take place there [7, 8]. If a metal is oxidized, the metal and oxygen can form a polarized dipole bond at the interface as shown in Fig. 2.6a. The M–O bonding can be described by the Mie-GrÜneisen potential energy $\phi(r)$ [9]:

$$\phi(r) = \frac{A}{r^m} - \frac{B}{r^n}, m > n, \tag{2.10}$$

where r is the distance between metal and oxygen, A and B are some constant values, m represents repulsive exponent and n is the attractive exponent. When a positive bias is applied across the interface, the polarization of the M–O bond will be distorted by the torque from the electric field. For example, when the dipole is in the same direction with the external field, the M–O bond will be stretched apart. The bond length increases from r_0 to r', and their Mie-GrÜneisen potential energy deviates from their most stable position, as shown in Fig. 2.6b. Overall, the barrier for bond breakage is reduced under an external field [10]. The breakage of M–O bonding will result in the metal-ion release into dielectrics [11–22].

Since metal-ion generation is attributed to M–O bond breakage, the energy barrier for ion generation is strongly related to the M–O bonding strength ($E_{m\text{-}o}$), as shown in Fig. 2.7. The M–O bonding strength is related to the heat of metal

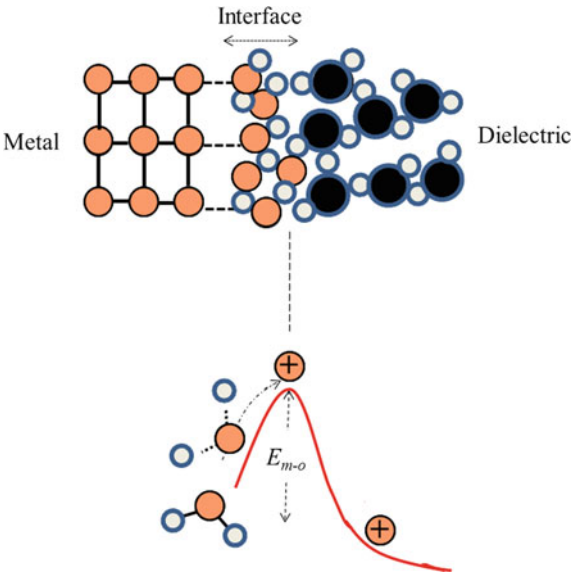

Fig. 2.7 An energy diagram for metal-ion generation at the metal–dielectric interface

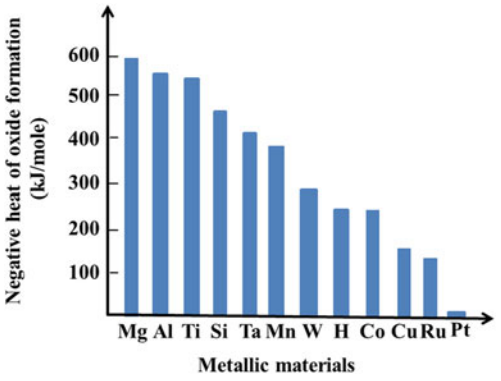

Fig. 2.8 The negative heat of oxide formation per oxygen atom is plotted for a selective group of metallic materials

oxide formation. A smaller negative heat of oxide formation implies a lower oxidation tendency and weaker M–O bonds, which may not be sustained under severe electrical and thermal stress. Figure 2.8 shows the negative heat of oxide formation per oxygen atom for a selective group of elements [23].

2.3.1 Pt−Dielectric Interface

Noble metals such as Pt have such a low negative heat of metal oxide formation that no metal oxide can be formed with Pt and no interface oxide layer exists between Pt and a dielectric. Meanwhile, Pt has a high melting temperature. Hence,

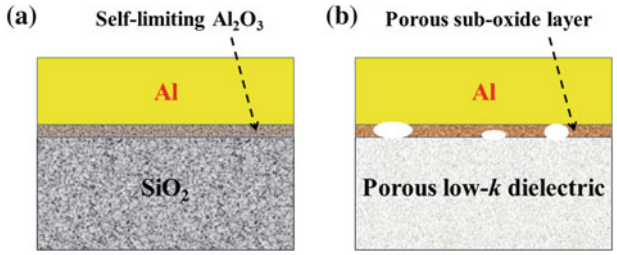

Fig. 2.9 **a** A cross-sectional schematic of an Al/SiO_2 structure, with the Al_2O_3 interface layer. **b** A cross-sectional schematic of an Al/porous low-*k* dielectric structure, with the porous Al sub-oxide layer at the interface

although there is no interface layer (with E_i) to halt Pt atom penetration, the metallic bonding (E_m) within Pt is strong enough to make it very thermally stable when deposited onto a dielectric surface. The lack of an interface oxide layer also eliminates ion generation, so there would be no Pt ion penetration under an external electric field. Solubilities of noble metals in dielectrics are negligibly small as well [24]. Therefore, noble metals such as Pt can serve as a reference against other metals for the study of metal penetration in dielectrics [18, 21]. Noble metals could also serve as electrodes to test intrinsic chemical stability factors such as the polarization effects of the dielectric itself under an external electric field [25].

2.3.2 Al−Dielectric Interface

Al has a low melting temperature, indicating a weaker E_m barrier. However, the negative heat of formation for Al_2O_3 is very high, 1677.4 kJ/mole (or 559 kJ/mole per oxygen atom). When Al is deposited on a SiO_2 surface, Al reduces SiO_2 to form a thin layer of Al_2O_3 as shown in Fig. 2.9a. This Al_2O_3 can serve as a barrier for two purposes. Firstly, it is so dense that it can prevent Al atoms or oxygen from diffusing through for further oxidation, acting as a so-called self-limited oxide. This capability is attributed to the high diffusion barrier (E_i) within the Al_2O_3 layer. Also, this dense Al oxide has very strong Al–O bonds (large $E_{m\text{-}o}$), which can prevent bond breakage in the oxide, eliminating the ion generation [26–28]. Therefore, Al-SiO_2 is a very stable interface and has served the microelectronic industry well for a long time.

However, when Al is deposited on a low-*k* dielectric, the situation can be very different. Most low-*k* dielectrics contain oxygen complexes, so Al oxide can be readily formed at the interface when Al is deposited onto these low-*k* dielectric surfaces. Very often, however, the density of oxygen in the low-*k* dielectric is not as abundant as that found in SiO_2, due to the porosity and other chemical ligands within the low-*k* material. Therefore, instead of a continuous layer of stoichiometic

Table 2.1 The negative heat of formation for metal oxides at 298.15 K in kJ/mole ($-\Delta H_f$) [23, 33–35]

Mg		Al		Ta		Ti		Ru	
MgO	601.2	Al_2O_3	1677.4	Ta_2O_5	2046.0	TiO	542.7	RuO_2	305.0
		$(AlO_2)^-$	823	TaO_2	180	Ti_2O_3	1520.9	RuO_3	78
		AlO(g)	−91.2	TaO	222	Ti_3O_5	2459.4	RuO_4	184.1
		Al_2O	130.0	Ta_3Si_5	335	TiO_2	944.0		
				Ta_2Si	125.5				
				$TaSi_2$	119.2				

W		Co		Mn		Cu		Si		H	
WO_2	589.7	CoO	238.9	MnO	384.9	CuO	155.2	SiO_2	910.4	H_2O	241.8
WO_3	842.9	Co_3O_4	905	MnO_2	520.1	Cu_2O	167.4	SiO	98.3	H_2O_2	187.8
				Mn_2O_3	956.9			SiH_4	30.5		
				Mn_3O_4	1386.6						

Al_2O_3, non-uniform Al sub-oxides (AlO_x) are formed, as illustrated in Fig. 2.9b. Table 2.1 shows the negative heat of oxide formation for a selective group of elements, including some sub-oxides [23]. Since the negative heat of formation for Al sub-oxides is not as large as that of Al_2O_3, they are not as stable. Al ions can be ripped apart from these sub-oxides under a strong electric field. Meanwhile, the sub-oxide layer could be porous and therefore unable to stop Al ion migration into the dielectric. As a result, unlike Pt, Al cannot be used as a standard reference to test the stability of metal/low-*k* dielectric interfaces [12, 17, 18, 21, 27, 28].

2.3.3 *Ta−Dielectric Interface*

Because Ta has a very high melting point indicating strong metal bonding (E_m), it is generally thermally stable on dielectric films without Ta atom diffusion under annealing. Furthermore, on a SiO_2 surface, Ta will react to form Ta_2O_5 and Ta silicide [29], which could act as a diffusion barrier against metal penetration. Therefore, Ta has been used as a reliable barrier for Cu-SiO_2 interconnect structures.

For porous low-*k* dielectrics, Ta/low-*k* dielectric interfaces are similar to those of Al/low-*k* dielectrics. When Ta is deposited on a low-*k* surface, Ta suboxides are created. The weakened Ta–O bonding in these suboxides serves as a source of ion generation under an electrical stress at an elevated temperature [14, 17, 18, 21, 30].

2.3.4 *Cu−Dielectric Interface*

As for Cu, its oxidation tendency is smaller than that of Al and Ta, but higher than that of Pt. The negative heat levels of oxide formation for CuO and Cu_2O per oxygen atom are 155.2 kJ/mole and 167.4kJ/mole, respectively. These are both

smaller than that of SiO_2, which is 455.2 kJ/mole. From the thermodynamic point of view, when Cu is deposited on a SiO_2 surface, it should not reduce the SiO_2 to form a Cu oxide. This fact was indeed verified by X-ray photoelectron spectroscopy (XPS) and internal photoemission [22, 31]. Thus, under an external electric field, no Cu ions should be generated at the Cu-SiO_2 interface, and no ion drift should occur. This was confirmed by electrical measurements in a contamination-free environment [22, 24]. However, Cu can be easily oxidized by residual moisture within the dielectric or by oxygen from the ambient environment. It is believed that most of the reports in the literature on Cu ion drift in SiO_2 result from the oxidation of Cu at the interface by the contamination of oxygen-containing species on the surface or from an oxidation ambient environment, instead of through the reduction of SiO_2 at the surface. So, in general, if there is a Cu oxide at the Cu-SiO_2 interface, Cu ions can be generated and released into SiO_2 under thermal or electrical stress.

Similarly, the interface of Cu on a low-*k* dielectric containing a SiO_x complex is stable against Cu ion generation if the interface is free from oxidant contamination. But this does not assure the Cu/low-*k* dielectric interface is more stable than that of interfaces of Al or refractory metals on low-*k* dielectrics. Cu has a relatively low melting temperature, which means its metallic bonding within Cu metal matrix is weak. Without a stable and dense interface, Cu atoms can diffuse thermally into low-*k* dielectrics at an elevated temperature or even during the physical vapor deposition of Cu [32].

2.4 Summary

The transport of metal-ions and atoms inside dielectrics under thermal or electrical stress can be well described once the diffusivity is known. However, the origin of the penetration of metal atoms and ions is complex. The metallic bonding and the quality of the interface layer will both affect metal atom diffusion from the interface into the dielectric. For metal-ions, we attempt to describe the generation and drift of metal-ions within a unifying picture based on thermochemistry that occurs at the interface which involves heat of formation, chemical reaction, and the energetics associated with physical transport. The interface oxide layer is the cause of metal-ions during stressing. A weak metal–oxide bonding can be broken apart under an electrical field at an elevated temperature, resulting in the release of metal-ions into dielectrics.

References

1. M.W. Hillen, J.F. Verwey, *Instabilities in Silicon Devices*, vol 1 (Elsevier, Amsterdam, 1986), p. 416
2. H. Mehrer, *Diffusion in Solids: Fundamentals, Methods, Materials, Diffusion-Controlled Processes* (Springer, New York, 2007), p. 27

3. A.S. Grove, *Physics and Technology of Semiconductor Devices* (Wiley, New York, 1967), p. 37
4. S.A. Campbell, *The Science and Engineering of Microelectronic Fabrication*, 2nd edn. (Oxford University Press, New York, 2001), p. 48
5. J.Y. Kwon, K.S. Kim, Y.C. Joo, K.B. Kim, Simulation of the copper diffusion profile in SiO_2 during bias temperature stress (BTS) test. Jpn. J. Appl. Phys. **41**, L99–L101 (2002)
6. M. Baklanov, K. Maex, M. Green, *Dielectric Films for Advanced Microelectronics* (Wiley, New York, 2007)
7. Y. Hirose, A. Kahn, V. Aristov, P. Soukiassian, V. Bulovic, S.R. Forrest, Chemistry and electronic properties of metal-organic semiconductor interfaces:Al, Ti, In, Sn, Ag, and Au on PTCDA. Phys. Rev. B **54**, 13748 (1996)
8. K. Nagao, J.B. Neaton, N.W. Ashcroft, First-principles study of adhesion at Cu/SiO_2 interfaces. Phys. Rev. B **68**(12), 125403 (2003)
9. P. Atkins, J.d. Paula, *Physical Chemistry*, 7th edn. (Freeman, San Francisco, 2002), p. 705
10. J.W. McPherson, H.C. Mogul, Underlying physics of the thermochemical E modelE model in describing low-field time-dependent dielectric breakdown in SiO_2 thin films. J. Appl. Phys. **84**, 1513–1523 (1998)
11. R.S. Achanta, W.N. Gill, J.L. Plawsky, G. Haase, Role of reactive surface oxygen in causing enhanced copper ionization in a low-k polymer. J. Vac. Sci. Technol. B **24**, 1417 (2006)
12. K.L. Fang, B.Y. Tsui, Metal drift induced electrical instability of porous low dielectric constant film. J. Appl. Phys. **93**, 5546–5550 (2003)
13. T. Fukuda, H. Nishino, A. Matsuura, H. Matsunaga, Force driving Cu diffusion into interlayer dielectrics. Jpn. J. Appl. Phys. **41**, 537 (2002)
14. M. He, Y. Ou, P.I. Wang, T.M. Lu, Kinetics of Ta ions penetration into porous low-k dielectriclow-k dielectrics under bias-temperature stress. Appl. Phys. Lett. **96**, 222901 (2010)
15. D. Kapila, J.L. Plawsky, Diffusion processes for integrated waveguide fabrication in glasses: a solid-state electrochemical approach. Chem. Eng. Sci. **50**, 2589 (1995)
16. A.L.S. Loke, R. Changsup, C.P. Yue, J.S.H. Cho, S.S, Wong, Kinetics of copper drift in PECVD dielectrics. IEEE Electron Device Lett. **17**, 549–551 (1996)
17. A. Mallikarjunan, S.P. Murarka, T.M. Lu, Mobile ion detection in organosiloxane polymer using triangular voltage sweep. J. Electrochem. Soc. **149**, F155 (2002)
18. A. Mallikarjunan, S.P. Murarka, T.M. Lu, Metal drift behavior in low dielectric constant organosiloxane polymer. Appl. Phys. Lett. **79**, 1855–1857 (2001)
19. S. Rogojevic, A. Jain, F. Wang, W.N. Gill, J.L. Plawsky, Interaction between silica xerogel and copper. J. Electrochem. Soc. **149**, F122 (2002)
20. S. Rogojevic, A. Jain, F. Wang, W.N. Gill, P.C. Wayner, J.L. Plawsky, T.M. Lu, G.R. Yang, W.A. Lanford, A. Kumar, H. Bakhru, N.A. Roy, Interactions between silican xerogel and tanatalum. J. Vac. Sci. Technol. B **19**, 354 (2001)
21. P.I. Wang, J.S. Juneja, Y. Ou, T.M. Lu, G.S. Spencer, Instability of metal barrier with porous methyl silsesquioxane films. J. Electrochem. Soc. **155**, H53 (2008)
22. B.G. Willis, D.V. Lang, Oxidation mechanism of ionic transport of copper in SiO_2 dielectrics. Thin Solid Films **467**, 284 (2004)
23. O. Kubaschewski, C.B. Alcock, *Metallurgical Thermochemistry*, 5th edn. (Pergamon Press, New York, 1979)
24. J.D. McBrayer, R.M. Swanson, T.W. Sigmon, Diffusion of metals in silicon dioxide. J. Electrochem. Soc. **133**, 1242–1246 (1986)
25. A. Mallikarjunan, S.P. Murarka, T.M. Lu, Separation of copper ion-induced and intrinsic polymer instabilities in polyarylether using triangular voltage sweep. J. Appl. Phys. **95**, 1216–1221 (2004)
26. I. Fisher, M. Eizenberg, Copper ion diffusion in porous and nonporous SiO_2-based dielectrics using bias thermal stress and thermal stress tests. Thin Solid Films **516**, 4111–4121 (2008)
27. M. He, H. Li, P.-I. Wang, T.M. Lu, Bias temperature stress of Al on porous low-k dielectriclow-k dielectrics. Microelectron. Reliab. **51**(8), 1342–1345 (2011)
28. A. Mallikarjunan, G.R. Yang, S.P. Murarka, T.M. Lu, Plasma surface modification for ion penetration barrier in organosiloxane polymer. J. Vac. Sci. Technol. B **20**, 1884 (2002)

29. M. Zier, S. Oswald, R. Reiche, M. Kozlowska, K. Wetzig, Interface formation and reactions at Ta-Si and Ta-SiO_2 interfaces studied by XPS and ARXPS. J. Elec. Spec. Relat. Phenom. **137–140**, 229–233 (2004)
30. T.L. Tan, C.L. Gan, A.Y. Du, C.K. Cheng, Effect of Ta migration from sidewall barrier on leakage current in Cu/SiOCH low-k dielectriclow-k dielectrics. J. Appl. Phys. **106**, 043517 (2009)
31. J.A. Kelber, C. Niu, K. Shepherd, D.R. Jennison, A. Bogicevic, Copper wetting of alpha-Al_2O_3(0001): theory and experiment. Surf. Sci. **446**, 76–88 (2000)
32. M. He, S. Novak, L. Vanamurthy, H. Bakhru, J. Plawsky, T.M. Lu, Cu penetration into low-k dielectriclow-k dielectric during deposition and bias-temperature stress. Appl. Phys. Lett. **97**(25), 252901 (2010)
33. E. Bauer, Epitaxy of metals on metals. Appl. Surf. Sci. **11–12**, 479–494 (1982)
34. E. Orhan, F. Tessier, R. Marchand, Synthesis and energetics of yellow TaON. Solid State Sci. **4**(8), 1071–1076 (2002)
35. W.M. Haynes (ed.), *CRC Handbook of Chemistry and Physics*, 91 edn. (CRC Press, Boca Raton, 2010)

http://www.springer.com/978-1-4614-1811-5

Metal-Dielectric Interfaces in Gigascale Electronics
Thermal and Electrical Stability
He, M.; Lu, T.-M.
2012, XI, 149 p., Hardcover
ISBN: 978-1-4614-1811-5